

Planar Array Infrared Spectroscopic Imaging of Monolayer Films in the 3200–2800 cm⁻¹ Region

Douglas L. Elmore* and Chad L. Leverette

Cargill Scientific Resources Center, Cordova, Tennessee 38016

D. Bruce Chase

*Central Research and Development, DuPont Experimental Station,
Wilmington, Delaware 19880-0328*

Anand T. Kalambur, Yujuan Liu, and John F. Rabolt

*University of Delaware, Department of Materials Science and Engineering,
Newark, Delaware 19716-3106*

Received October 31, 2002. In Final Form: January 27, 2003

The ability of a planar array infrared (PA-IR) spectrograph to obtain spatially resolved infrared spectra (infrared line images) of a monolayer film with reasonable signal-to-noise-ratios is demonstrated, and the first infrared line images of a monolayer film ever recorded are reported. In this context, octadecyltrichlorosilane (OTS) monolayer films self-assembled on glass substrates were investigated as a function of three different solvents (hexane, benzene, and toluene). It is shown that the PA-IR line images could be used to investigate surface coverage and conformational order as a function of spatial location. A frequency versus absorbance relationship was observed that can be interpreted as a well-defined correlation between conformational order and surface coverage. The plot of this relationship, which looks similar to a phase diagram containing a first-order phase transition, is in excellent agreement with that reported recently (Liu, Y.; Wolf, L. K.; Messmer, M. C. *Langmuir* 2001, 17, 4329) by sum frequency generation (SFG). On the basis of the results from this study and the SFG results, it appears that conformational order and surface coverage of self-assembled OTS monolayer films on glass can be treated as two dependent thermodynamic state functions. In addition, these results suggest that different solvent systems can be exploited to tailor self-assembled monolayer films in terms of surface coverage and conformational order.

Introduction

Organic monolayer films^{2,3} enjoy a large number and diverse scope of applications. A few of these include semiconductor and sensor coatings,^{4–6} nanolithography,^{7,8} and model biological systems.⁹ For this reason, monolayer films have received and continue to receive considerable attention in both fundamental and applied research.

Fourier transform infrared (FT-IR) spectroscopy has been used to study spatially averaged monolayer films assembled on both metallic and dielectric substrates.^{10–12} This spectroscopic technique can be used to probe surface density, conformational order, and molecular orientation.

More recently, interest has grown in the ability of FT-IR imaging to provide spatially resolved spectra^{13–18} of bulk materials, and in theory, FT-IR imaging systems could be used to investigate monolayer films. Unfortunately, to date, these systems have not provided the necessary sensitivity for monolayer analysis.^{19,20} Elmore et al.²¹ recently showed that broadband infrared spectra with very low noise levels can be obtained using a planar array infrared spectrograph (PA-IR spectrograph). Using a focal plane array, the ultrasensitive, high-speed PA-IR instrument can easily record the IR spectrum of a monolayer in matter of seconds with an acceptable signal-to-noise ratio (SNR). In this paper, we demonstrate that a PA-IR spectrograph can be used to obtain spatially resolved spectra of a monolayer film. To our knowledge, these are the first reported broadband infrared images of monolayer films.

* To whom correspondence should be addressed. Office: (901) 775–5945. Fax: (901) 937-4531. E-mail: Doug_Elmore@cargill.com.

(1) Liu, Y.; Wolf, L. K.; Messmer, M. C. *Langmuir* 2001, 17, 4329.
(2) Ulman, A. *An Introduction to Ultrathin Organic Thin Films. From Langmuir Blodgett to Self-Assembly*; Academic Press: San Diego, 1991.
(3) Ulman, A. *Chem. Rev.* 1996, 96, 1533.
(4) Angst, D. L.; Simmons, G. W. *Langmuir* 1991, 7, 2236.
(5) Willner, I.; Schlittner, A.; Doron, A.; Joselevich, E. *Langmuir* 1999, 15, 2766.
(6) Allara, D. *Biosens. Bioelectron.* 1995, 10, 771.
(7) Komeda, T.; Namba, K.; Nishioka, Y.; Namba, K.; Nishioka, Y. *J. Vac. Sci. Technol.* 1998, 3, 1680.
(8) Jeon, N. L.; Finnie, K.; Branshaw, K.; Nuzzo, R. G. *Langmuir* 1997, 13, 3382.
(9) Dluhy, R. A.; Stephens, S. M.; Widayati, S.; Williams, A. D. *Spectrochim. Acta, Part A* 1995, 51, 1413.
(10) Greenler, R. G. *J. Chem. Phys.* 1966, 44, 310.
(11) Rabolt, J. F.; Burns, F. C.; Schlotter, N. E.; Swalen, J. J. *Chem. Phys.* 1983, 78, 946.
(12) Brunner, H.; Mayer, U.; Hoffman, H. *Appl. Spectrosc.* 1997, 51, 209.

(13) Lewis, E. N.; Treado, P. J.; Reeder, R. C.; Story, G. M.; Dowrey, A. E.; Marcott, C.; Levin, I. W. *Anal. Chem.* 1995, 67, 3377.
(14) Lewis, E. N.; Gorbach, A. M.; Marcott, C.; Levin, I. W. *Appl. Spectrosc.* 1996, 50, 263.
(15) Bhargava, R.; Levin, I. W. *Anal. Chem.* 2001, 73, 5157.
(16) Marcott, C.; Reeder, R. C.; Paschalis, E. P.; Tatakis, D. N.; Boskey, A. L.; Mendelsohn, R. *Cell. Mol. Biol.* 1998, 44, 109.
(17) Snively, C. M.; Koenig, J. L. *Macromolecules* 1998, 31, 3753.
(18) Mendelsohn, R.; Paschalis, E. P.; Boskey, A. L. *J. Biomed. Opt.* 1999, 4, 14.
(19) Bhargava, R.; Ribar, T.; Koenig, J. L. *Appl. Spectrosc.* 1999, 53, 1313.
(20) Bhargava, R.; Wang, S. Q.; Koenig, J. L. *Appl. Spectrosc.* 2000, 54, 486.
(21) Elmore, D. L.; Tsao, M. W.; Frisk, S.; Chase, D. B.; Rabolt, J. F. *Appl. Spectrosc.* 2002, 56, 145.

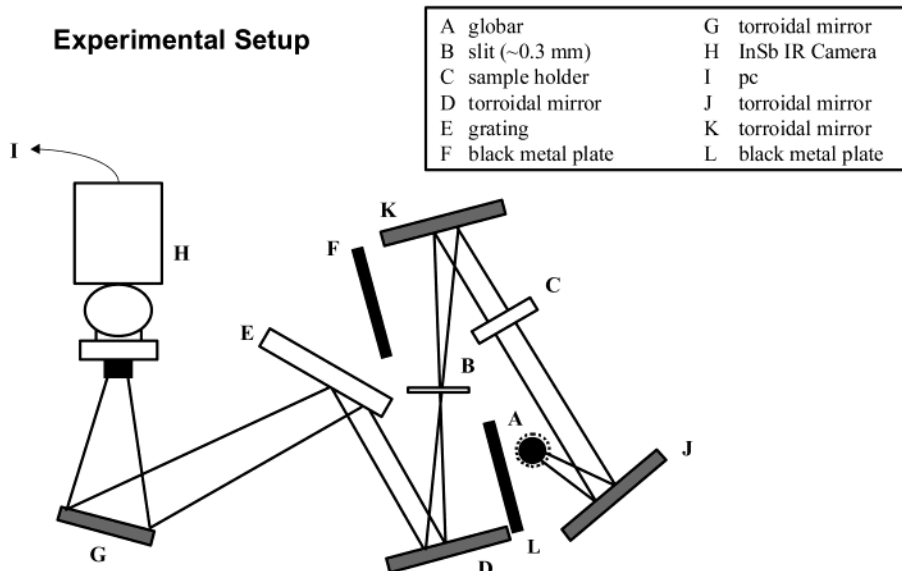


Figure 1. Experimental arrangement of components in the PA-IR spectrograph.

Specifically, we use the PA-IR spectrograph to investigate the effect of solvent on the surface coverage and the conformational order of an *n*-octadecyltrichlorosilane (OTS) monolayer film self-assembled on a glass substrate.²² The quality of an organosilane self-assembled monolayer (SAM) film is highly dependent on the reaction conditions, including the choice of solvent.²³ In this work, the solvent effect is further explored by exploiting the PA-IR spectrograph's ability to provide spatially resolved information describing conformational order and surface coverage.

Experimental Section

Materials and Reagents. OTS was obtained from Aldrich at 90+% purity. Toluene (HPLC grade), hexane (HPLC grade), and benzene (ACS grade) were obtained from Fisher Scientific. The solvents used in the cleaning process were 30% H₂O₂, 37.8% HCl, and 29.8% NH₄OH (all certified ACS grade, Fisher Scientific). All chemicals listed above were used without further purification. Ultrapure water (resistivity of 18.2 MΩ cm, Millipore Ultrapure water system, Millipore Inc.) was used throughout the cleaning procedure.

Pretreatment of Surfaces. Plain glass microscope slides (3 in. × 1 in., Fisherbrand, Fisher Scientific) were cleaned according to a standard procedure.²⁴ The slides (five slides per cleaning batch) were immersed in a NH₄OH/H₂O₂/H₂O (1:1:5) solution at 65 °C for 15 min, rinsed in water for 10 min, immersed in a HCl/H₂O₂/H₂O (1:1:5) solution at 65 °C for 15 min, rinsed in water for 10 min, and finally dried in a flow of warm, clean nitrogen gas. One of the cleaned slides was immediately stored under nitrogen and used for collecting the reference IR spectra.

Preparation of the Monolayers. OTS solutions were prepared at 1 mM concentration under a nitrogen atmosphere and used immediately. The cleaned slides were immersed into vials containing the freshly prepared solutions and sealed with Parafilm under nitrogen. The coated slides were then taken out after an hour, rinsed using the respective solvents, and dried using warm nitrogen.

PA-IR Spectrograph. A block diagram of the PA-IR spectrograph is presented in Figure 1. Broad band infrared radiation produced by a global is collected and collimated with a torroidal mirror (*f*/2.5) and directed through a sample holder. The light is focused on an adjustable slit with a second torroidal mirror and then reflected by a third torroidal mirror. The light is then

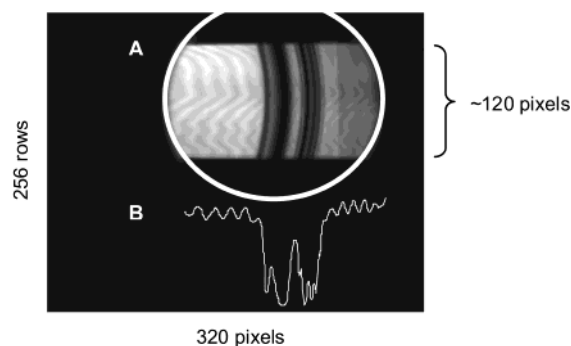


Figure 2. (A) A spectral image of a polystyrene film and (B) a corresponding transmittance spectrum obtained from a single pixel row.

diffracted by a ruled grating (rotatable), reflected off a fourth torroidal mirror, and finally collected (with *f*/2.3 condensing optics) and focused onto an InSb 320 × 256 focal plane array (FPA) detector cooled with liquid nitrogen. All four torroidal mirrors are matched. Camera optics include a 3–5 μm band-pass filter for noise reduction. The global used in this instrument was ~3 cm high with a diameter of ~10 mm and was driven by a regulated power supply. A resolution element, defined by the pixel size, was approximately 5 cm⁻¹. Other aspects of the spectrograph have been described previously.²¹

A two-point nonuniformity correction of the FPA response was performed at the beginning of the study with a 1.5 ms integration time using ~75% of the camera's dynamic range. One-point nonuniformity corrections were performed prior to data acquisition. The method for performing both corrections has previously been described.²¹

Raw spectral data files were collected and saved as 320 × 256 images (TIF) using Image-Pro Plus software (Media Cybernetics, Silver Spring, MD) and a personal computer with a 650 MHz processor and 256 MB of RAM. The frame rate was 60 frames/s, limiting the minimum total acquisition time to 17 ms.

Spectral Images. Figure 2 shows a slit image dispersed across the FPA (spectral image) with a polystyrene (PS) film placed in the sample position of the PA-IR spectrograph described by Figure 1. The light color indicates areas of high signal intensity, while the dark color indicates areas of low signal intensity corresponding to the strong spectral absorbances observed for PS in the ~3200–2800 cm⁻¹ region. The spectral image is about 100 pixel rows high and about 200 pixels wide. The height of the image is determined by the height of the global light source (the global height is less than the slit height) and the monochromator optics. The width is limited by the diameters of the optics (mirrors,

(22) Sagiv, J. *J. Am. Chem. Soc.* **1980**, *102*, 92.

(23) McGovern, M. E.; Kallury, K. M. R.; Thompson, M. *Langmuir* **1994**, *10*, 3607.

(24) Kern, W.; Puotinen, D. A. *RCA Rev.* **1970**, 187.

grating, etc.). All infrared line images presented in this paper were obtained by averaging 1600 frames. The total acquisition time was about 27 s.

Spatially resolved spectra are obtained from the individual pixel rows. As an example, a transmittance spectrum of PS obtained from a single row of the spectral image is superimposed at the bottom. Note the familiar absorbance bands observed in the spectral image. Each pixel row corresponds to a distance of 300 μm along the sample holder. Note how the unevenness of the PS film shifts the interference fringes back and forth in frequency from row to row, clearly demonstrating the ability of a PA-IR spectrograph to provide spatially resolved spectra.

PA-IR Spectra. Ratioed spectra were calculated using Excel (Microsoft, Redmond, WA) as previously described.²¹ The spectra were plotted using GRAMS/32 (Galactic Industries, Salem, NH).

Normalization. Note in Figure 2 how the spectral absorbances shift in an arclike pattern as individual pixel rows are observed from the top to the bottom of the line image. This effect is commonly referred to as "slit curvature" and is dependent on the f -number of the monochromator. To eliminate the slit curvature, the pixel numbers for each individual row are normalized against the first pixel row in the line image (with a sample placed in the sample holder). In other words, the intensity versus pixel number plot for each pixel row is calibrated against the intensity versus pixel number plot of the first row in the line image, and the observed peaks in each pixel row are forced to line up at the same pixel column number. This is equivalent to a row-dependent frequency shift that corrects for the optical slit curvature.

Signal Averaging of Spatially Resolved Spectra. All spectra presented in this paper were obtained by signal averaging four pixel rows. The signal averaging was performed prior to determination and application of the normalization function. The signal averaging was performed first to reduce the data reduction time. As a result, the accuracy of spectra is slightly compromised. However, the error, which is constant, is observed as a slight degradation in spectral resolution. After this initial averaging, the number of spectra is reduced from 100 to 25.

Frequency Calibration. Frequencies in the PA-IR spectra were calibrated using a method previously described.²¹ Frequency values with $\leq 0.2 \text{ cm}^{-1}$ error were obtained with this method in the region of interest ($\sim 2950\text{--}2900 \text{ cm}^{-1}$).

Spatial and Spectral Resolution. As discussed earlier, for each line image, four spectra (four pixel rows) with a spatial resolution of 300 μm each were signal averaged resulting in a final spatial resolution of 1.2 mm defined by a line spectrum. Each line image was then produced from 28 spatially resolved signal averaged spectra and thus corresponds to a distance of $28 \times 1.2 \text{ mm} = 3.4 \text{ cm}$. The spectral resolution at $\sim 2920 \text{ cm}^{-1}$ was about 6 cm^{-1} as determined by comparison of PA-IR and FT-IR spectra.

Results and Discussion

OTS monolayer films were self-assembled on three equivalent glass substrates using benzene, hexane, and toluene as solvents. The same films were then prepared three more times for a total of four separate replicate sample sets. A PA-IR spectrograph was then used to obtain spatially resolved infrared spectra of these monolayer films.

As an example, a monolayer spectrum is presented in Figure 3A. This spectrum corresponds to an OTS monolayer that was self-assembled using hexane as a solvent. Numerous assignments can be made and include the $\nu_a(\text{CH}_2)$ band ($\sim 2920 \text{ cm}^{-1}$), the $\nu_s(\text{CH}_2)$ band ($\sim 2850 \text{ cm}^{-1}$), and the $\nu_a(\text{CH}_3)$ band ($\sim 2960 \text{ cm}^{-1}$). The $\nu_s(\text{CH}_3)$ vibration ($\sim 2870 \text{ cm}^{-1}$) is observed as a shoulder on the $\nu_s(\text{CH}_2)$ band, while the $\nu_a(\text{CH}_2)$ band shape is complicated due to overlapping contributions from broad Fermi resonance bands.^{25,26} It has been shown previously that the frequen-

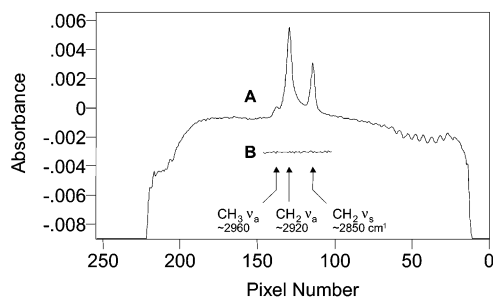


Figure 3. (A) A spatially resolved, single spectrum (an average spectrum derived from four contiguous pixel rows) of a self-assembled OTS monolayer on a glass substrate produced using hexane as a solvent and (B) the corresponding 100% line for the same spectral region.

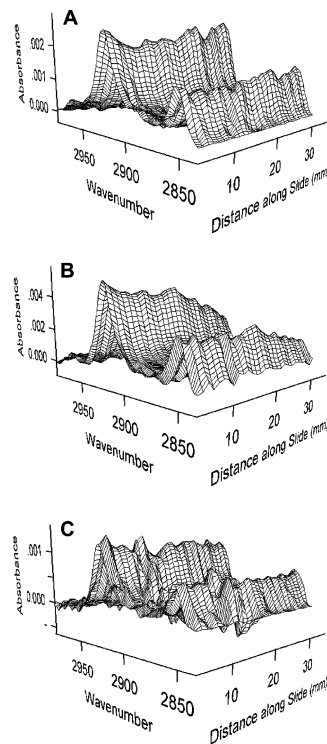


Figure 4. Line images of self-assembled OTS monolayers on a glass substrate produced using (A) benzene, (B) hexane, and (C) toluene. All three plots are scaled to the largest absorbance value; note the significant difference in the absorbance maximum from plot to plot.

cies of both the $\nu_a(\text{CH}_2)$ and $\nu_s(\text{CH}_2)$ bands can be used to qualitatively monitor the conformational order of alkyl chains.²⁵ The $\nu_s(\text{CH}_2)$ band is usually chosen over the $\nu_a(\text{CH}_2)$ to avoid complications due to Fermi resonance. However, the $\nu_a(\text{CH}_2)$ band appears in the spectrum with the highest SNR and for this reason was used to monitor both surface coverage and conformational order in this study.

A 100% line for the C–H stretching region was produced by ratioing the spectra of two clean glass slides and is presented in Figure 3B (below the OTS monolayer spectrum). The line shows that the glass slides are free of detectable contamination in this region, and the noise level is less than 150 microabsorbance units. For reference purposes, the SNR of the band at 2920 cm^{-1} is $\sim 50:1$ in Figure 3A.

An example of spatially resolved spectra (line images) for each of the three solvent systems is presented in Figure 4A–C. The spatial resolution is 1.2 mm. Each line image

(25) Snyder, R. G.; Hsu, S. L.; Krimm, S. *Spectrochim. Acta, Part A* **1978**, *34A*, 395.

(26) Snyder, R. G.; Strauss, H. L.; Elliger, C. A. *J. Phys. Chem.* **1982**, *86*, 5145.

contains 28 spectra and thus corresponds to a distance of 3.4 cm.

Depending on the sampling configuration and the state of the monolayer, absorbance values can be used to monitor surface density or molecular orientation.¹¹ In the case where orientation effects are negligible, absorbance values are proportional to the molecular density and are therefore a direct measure of monolayer coverage. In this study, the glass substrate was always held at an angle of 20° relative to the incident beam. At this angle, the orientation effects are reduced. Furthermore, the magnitudes of the changes in the absorbance values considered in this paper are large enough that the effect of orientation can be neglected.

When the line images in Figure 4A–C are compared, it is observed that the average absorbance of the $\nu_a(\text{CH}_2)$ band for the hexane system (~4 milliabsorbance units (mA)) is twice that observed for the benzene system (~2 mA) and 4 times that found for toluene (~1 mA). Since an absorbance value of 4–5 mA²⁷ is consistent with the literature for an ordered OTS monolayer film on a dielectric substrate,^{28,29} certain conclusions can be drawn from our observations. Deposition of OTS from hexane produced approximately one full monolayer on the glass, while deposition from benzene produced domains that, on the average, covered 50% of the glass surface. Correspondingly, about 25% of the glass substrate is covered with monolayer domains when OTS is deposited from toluene.

Some simple statistics are useful for a more quantitative comparison of all 12 samples. It is interesting to note that the average absorbance is proportional to surface density (orientation effects are neglected) and can therefore be used as a measure of surface coverage. Furthermore, the relative standard deviation (RSD) of the spatially resolved absorbance values in a line image is a direct measure of the relative variation in surface density across the slide and therefore reflects the spatial heterogeneity of the monolayer film in terms of surface coverage. The average frequency of the $\nu_a(\text{CH}_2)$ band is a qualitative measure of the conformational order of the alkyl chains in the monolayer. The standard deviation of the frequency of the $\nu_a(\text{CH}_2)$ band is a direct measure of the variation in conformational order across the slide and therefore reflects the spatial conformational heterogeneity of the monolayer film. These statistical values have been determined for all 12 samples and are presented in Table 1.

As shown in Table 1, OTS deposition from hexane consistently produced monolayer films with the highest surface coverage (largest average absorbance of 0.004 80) and the most ordered alkyl chains (lowest average frequency (2919.0 cm⁻¹) of the $\nu_a(\text{CH}_2)$ band). OTS from hexane ranked second in terms of variation in conformational order across the slide with an average standard deviation of 1.12 cm⁻¹ (really about the same as benzene (1.07 cm⁻¹) when accounting for error). Interestingly though, with an average RSD of 12.4, OTS deposited from hexane produced the most heterogeneous surface coverage.

Both self-assembled and Langmuir monolayer films of OTS form islandlike domains in this condensed state.^{2,30,31} It seems quite reasonable that the molecular

Table 1. Band Frequency and Absorbance Values for OTS Monolayer Films on Glass Substrates as a Function of Solvent

sample		frequency (cm ⁻¹) ^a	standard deviation ^b	absorbance ^c	RSD of absorbance values (%) ^d	
benzene	set	1	2919.96	0.62	0.002 30	8.3
		2	2919.32	1.08	0.002 86	5.2
		3	2919.56	1.28	0.002 67	6.0
		4	2920.12	1.30	0.002 28	10.0
hexane	set	1	2919.80	0.69	0.004 00	17.8
		2	2918.95	1.16	0.004 81	14.8
		3	2918.58	1.47	0.005 00	11.4
		4	2918.50	1.14	0.005 40	5.6
toluene	set	1	2923.88	2.23	0.000 98	11.2
		2	2922.36	1.57	0.001 23	6.5
		3	2919.50	1.05	0.002 24	4.0
		4	2919.49	1.33	0.002 47	6.1

^a Represents the frequency (cm⁻¹) of the CH₂ ν_a (mean) of an OTS monolayer prepared with either benzene, hexane, or toluene. Four sample sets were separately prepared and analyzed. Frequencies of the CH₂ ν_a bands are qualitative indicators of conformational order. ^b Standard deviations for the frequencies obtained from the CH₂ ν_a reflect spatial variations in conformational order. ^c Absorbance values (mean) calculated from the peak height of the baseline-corrected CH₂ ν_a . These values are proportional to surface coverage (when orientation effects are neglected). ^d Relative standard deviation (RSD) of the absorbance values from the CH₂ ν_a reflect spatial variations in surface coverage.

coverage inside a monolayer domain is fairly homogeneous while the distribution of the domains across the slide could be more heterogeneous, especially on an ordinary glass slide. This claim is supported by these RSD values for the monolayers prepared from hexane. The RSD values systematically decrease from 17.8 to 5.6 as the absorbance values increase from 0.004 00 to 0.005 40 (74–100% surface coverage).

Benzene consistently produced about one-half of a monolayer film with an average absorbance of 0.002 53. With an average RSD of 7.38, benzene ranked second in terms of homogeneous surface coverage. The alkyl chains in these films were slightly more disordered than the hexane films with an average frequency of 2919.7 cm⁻¹. Benzene produced the most homogeneous films in terms of variation in conformational order across the slide with an average standard deviation of 1.07 cm⁻¹.

OTS from toluene produced films that had the lowest surface coverage (ranging from 18 to 46%) and an average absorbance of 0.001 73. Interestingly, OTS from toluene also produced the most homogeneous films in terms of surface coverage with an average RSD of 6.95. It seems reasonable that the OTS films prepared with toluene appear more homogeneous than those prepared with hexane, and this can be partially explained by the absence of islandlike domains. Note that the film with the highest surface coverage had a very homogeneous coverage (RSD of 5.6) which compares well with the surface coverage variation for the films prepared with toluene (RSD of 6.95).

OTS from toluene produced films with the most disordered alkyl chains with an average $\nu_a(\text{CH}_2)$ frequency of 2921.3 cm⁻¹ which ranged from 2919.5 to 2923.9 cm⁻¹. Also note that the OTS film produced in set 1 using toluene showed the most conformational disorder with a frequency of 2923.9 cm⁻¹ and the greatest variation in conformational disorder with a standard deviation of 1.55 cm⁻¹. It is clear that the variation in conformational disorder is not controlled solely by choice of solvents but involves other yet undefined experimental parameters.

(27) Note that the absorbance value actually corresponds to two monolayers since both sides of the glass slide are covered with a monolayer film.

(28) Parikh, A. N.; Allara, D. L.; Azouz, I. B.; Rondelez, F. *J. Phys. Chem.* **1994**, *98*, 7577.

(29) Allara, D. L.; Parikh, A. N.; Rondelez, F. *Langmuir* **1995**, *11*, 2357.

(30) Davidovits, J. V.; Pho, V.; Silberzan, P.; Goldmann, M. *Surf. Sci.* **1996**, *352–354*, 369.

(31) Lercel, M. J.; Tiberio, R. C.; Chapman, P. F.; Craighead, H. G.; Sheen, C. W.; Parikh, A. N.; Allara, D. L. *J. Vac. Sci. Technol., B* **1993**, *11*, 2823.

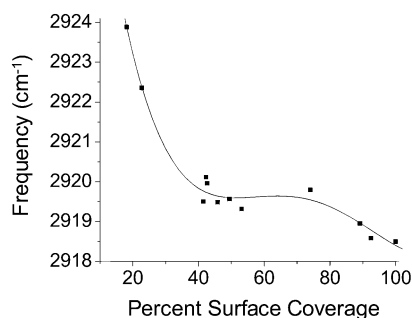


Figure 5. Frequency of CH₂ versus monolayer coverage with 100% surface coverage defined by the largest hexane absorbance.

It is important to note that the SNRs of the spectra reported in this paper are limited and overinterpretation should be avoided. However, it is clear that higher SNRs can be obtained conveniently if some form of in-scan coaddition is employed for signal averaging in order to free up computer memory. This feature will significantly increase the nonstop data acquisition time from a fraction of a minute to literally hours. Future work on the next generation PA-IR instrument is addressing this issue.

Finally, a well-defined relationship is observed between frequency and absorbance that appears to be independent of the solvent used for deposition. Since absorbance is directly proportional to surface density (if orientation effects can be neglected), it is clear that the choice of solvent has a large influence on the amount of surface coverage. Since a change in band frequency is indicative of a change in conformational order in the alkyl chains, it appears that the conformational order is a function of surface coverage. In general, the results are in good agreement with those recently reported by Liu et al.¹

A plot of frequency (a measure of conformational order) versus surface coverage is presented in Figure 5. Surface coverage values were determined by normalizing all the absorbance values against the largest absorbance value observed in the study (set 4, hexane); that is, we assumed that the largest absorbance value corresponded to 100% surface coverage. The data points have been fit with a fourth-order polynomial to emphasize the trend.

Interestingly enough, the plot resembles a frequency–area isotherm of a Langmuir monolayer determined with a Langmuir film balance and an infrared spectrometer.³² For the sake of discussion, we will treat the plot as a phase diagram in which surface coverage is the independent variable and band frequency is the dependent variable. However, the reader should keep in mind that different surface coverages correspond to self-assembled films obtained from different solvents.

On the basis of a large change in frequency from about 2924 to 2920 cm⁻¹, a disorder-to-order phase transition takes place somewhere between 18 and 40% surface coverage. Frequency values of the $\nu_a(\text{CH}_2)$ stretching band ranging from 2920.2 to 2919.3 cm⁻¹ are observed between 40 and 89% OTS coverage. This region of relatively constant frequency near 2920 cm⁻¹ suggests the existence of an ordered phase. A possible second phase transition is observed near 89% coverage where the frequency values change rapidly again. On the basis of the frequencies, this region may correspond to some type of solid–solid phase transition. It is important to note that for this region, the IR measurements are most sensitive to orientation effects; that is, as the surface coverage approaches 100%, the OTS alkyl chains exist in a mostly all-trans (zigzag)

conformation with only a small amount of conformational disorder. If the effect of orientation is significant, it would appear as an increase in the absorbance value¹¹ (in addition to the increase in absorbance due to increase in surface density). The result would elongate the second transition region in Figure 5. In other words, a sharper transition should be observed if the orientation effects could be completely eliminated. Finally, it is likely that the last two data points at ~93 and 100% surface coverage both lie on the plateau of a second condensed phase corresponding to the crystalline phase 1.

Most recently, Liu et al.¹ reported a similar conformational order versus surface coverage plot using adsorption-time-dependent sum frequency generation (SFG) spectra (to determine conformational order) and contact angle measurements (to measure surface coverage). Within the limitations of the measurements, the “transition” and “phase” regions reported by Liu et al. are essentially identical to those reported in Figure 5. The excellent agreement in results serves to validate the PA-IR spectrographic method described here. The fact that the adsorption-time-dependent data agree so well with the solvent-dependent data in our work suggests that Figure 5 describes a history-independent relationship between two thermodynamic state functions. Finally, from a method standpoint, it should be noted that unlike SFG,³³ PA-IR spectrographs can be used to obtain spatially resolved information about both conformational order and surface coverage directly from monolayer films assembled on dielectric substrates.

The results described in this paper also suggest that it may be possible to tailor surface coverage and conformational order using different solvent systems. Of specific interest is the possibility for a second component to be assembled in the “holes” left using benzene or toluene as a solvent. The result would be a phase-separated two-component monolayer film with unique properties. Future work will be pursued in this area.

Conclusions

A PA-IR spectrograph can be used to obtain infrared line images of monolayer films with good SNRs. These line images can be used to investigate surface coverage and conformational order in the spatial domain. On the basis of the results from this study, hexane can be used to consistently produce OTS monolayer films with high surface coverage. Benzene can be used to consistently produce approximately 50% of a monolayer with a relatively homogeneous surface coverage (more homogeneous than the hexane). Toluene can be used to produce OTS monolayer films with relatively low surface coverage, in some cases less than 20% of a monolayer. Fairly heterogeneous surface coverages are observed for films prepared with hexane that had 93% or less surface coverage. This observation may be explained by the formation of islandlike domains in the condensed state monolayer. Specifically, while the molecule to molecule arrangement in the monolayer is reasonably homogeneous, the domain to domain spatial arrangement is quite heterogeneous. When all 12 data sets were considered, a well-defined frequency versus absorbance relationship was observed. The plot of this relationship, which can be interpreted as conformational order (frequency) versus surface coverage (absorbance), is in excellent agreement with the literature. The fact that the adsorption-time-

(32) Dluhy, R. A.; Cornell, D. G. *ACS Symp. Ser.* **1991**, *447*, 192.

(33) Shen, Y. R. *Nature* **1989**, *337*, 519.

dependent data from SFG spectra by Liu et al.¹ agree so well with the solvent-dependent data in this work strongly suggests that Figure 5 describes the history-independent relationship between two thermodynamic state functions. The results of this study also suggest that different solvent systems can be used to tailor self-assembled monolayer films in terms of surface coverage and conformational order. Future work will include determinations of spatially

resolved molecular orientations in monolayer films deposited on metallic substrates.

Acknowledgment. The author gratefully acknowledge DOE-PAIR (DE-FG02-99-ER45794), NSF-DMR (9812088), and NSF-SGER-CHEM (0228839) for partial support during the course of this work.

LA0208878